Enzyme Reactions in Nanoporous, Picoliter Volume Containers

Piro Siuti[a], **Scott T. Retterer**[b,c], **Chang-Kyoung Choi**[c,d], and **Mitchel J. Doktycz**[a,b,c]

[a]University of Tennessee-Oak Ridge National Laboratory, Graduate School of Genome Science and Technology, Knoxville, TN 37996 USA

[b]Biosciences Division, Oak Ridge National Laboratory, Oak Ridge, TN 37831, USA

[c]Center for Nanophase Materials Sciences, Oak Ridge National Laboratory, Oak Ridge, TN 37831, USA

[d]Mechanical Engineering-Engineering Mechanics, Michigan Technological University, Houghton, MI 49931-1295, USA

Abstract

Advancements in nanoscale fabrication allow creation of small volume reaction containers that can facilitate the screening and characterization of enzymes. A porous, ~19 pL volume vessel has been used in this work to carry out enzyme reactions under varying substrate concentrations. Assessment of small molecule and Green Fluorescent Protein diffusion from the vessels indicates that pore sizes on order of 10 nm can be obtained, allowing capture of proteins and diffusive exchange of small molecules. Glucose oxidase and horseradish peroxidase can be contained in these structures and diffusively fed with a solution containing glucose and the fluorogenic substrate Amplex Red™ through the engineered nanoscale pore structure. Fluorescent microscopy was used to monitor the reaction, which was carried out under microfluidic control. Kinetic characteristics of the enzyme (K_m and V_{max}) were evaluated and compared with results from conventional scale reactions. These picoliter, nanoporous containers can facilitate quick determination of enzyme kinetics in microfluidic systems without the requirement of surface tethering and can be used for applications in drug discovery, clinical diagnostics and high-throughput screening.

INTRODUCTION

Enzymes are responsible for catalyzing and increasing the reaction rates of almost all biochemical reactions that occur inside and outside of biological cells. They are also broadly used for applications involving sensing and material processing [1,2]. Consequently, a high priority is placed on optimizing and understanding enzyme activity. Often, this requires time consuming structural determinations and genetic engineering [2-4]. New approaches for biochemical assessment are also essential. A key challenge in optimizing and characterizing biocatalysts is overcoming the impracticality of conventional enzyme screening techniques. Large amounts of sample are often required and only a limited number of variants can be characterized at one time. Miniaturized reaction systems can overcome these issues and further relieve the need for mixing, potentially decreasing analysis times [1]. These advantages can facilitate enzyme kinetic studies and enable the screening of combinations of enzyme and substrates in a parallel manner [1,5-7], resulting in a more rapid determination of the affinity of substrates or inhibitors as required for evaluating new drug candidates [1,8].

CORRESPONDING AUTHOR M. J. Doktycz is with the Biosciences Division and the Center for Nanophase Materials Sciences, Oak Ridge National Laboratory, Oak Ridge TN 37831-6445 and the University of Tennessee, Knoxville. (corresponding author, phone: 865 574-6204, fax 865 241-4579, doktyczmj@ornl.gov).

Advances in micro- and nanotechnology have enabled the engineering of systems at greatly reduced scale [9] and have led to new approaches for creating enzyme microreactors [10]. Various formats and materials have been considered [11-14]. Commonly, microdevices for biosensing and enzyme kinetic analyses have focused on miniaturizing the reaction container [7]. For example, techniques for creating multiple microreactors in micrometer-size glass capillaries or in microfabricated channels have been described and used to facilitate the study of enzyme kinetics under different values of temperature and/or pH [15-17]. Miniaturization that allows for analyses at the level of single enzyme molecules has also been described [18]. Microfluidic-based formats can facilitate automation and monitoring. Pioneering efforts for microfluidic based analyses of enzyme kinetics involved electrokinetic transport of reagents and samples to control dilution and mixing. This approach demonstrated reduced enzyme and substrate consumption over conventional methods [19]. Stopped-flow enzyme assays that employed microfabricated mixers [20] and centrifugal microfluidic system have also been described [21]. Many of these approaches operate essentially in a "batch mode" and are unable to remove inhibitory byproducts [8] or dynamically change reaction conditions. Further, depending on the reaction volume, reaction mixing can be a concern [1,7,8,16].

An alternate approach is to operate in a "continuous mode", where reactants are fed and products removed. Miniaturized versions of this approach can prevent buildup of inhibitory byproducts and allow for assay automation while also reducing time and reagent consumption. A common approach to implementing microscale continuous mode designs involves immobilization of the enzyme onto a solid support for a continuous or stopped-flow analysis of enzyme kinetics [7,22-26]. However, a limitation of these previous microreactors is the inability to precisely define and control the transport of different sized molecules [7]. Further, immobilizing enzymes onto solid surfaces can be a drawback as damage or alteration of enzyme structure can result leading to potential changes in intrinsic kinetic rate characteristics or loss of activity [22]. Many of these shortcomings can be addressed by designing devices with pores small enough to contain the enzymes in their native structure and large enough to allow transport of substrates and inhibitory byproducts.

Reported here is a microfluidically addressable, nanoporous, picoliter volume container for carrying out enzymatic reactions (**Fig. 1**). The system operates under continuous flow and facilitates measurement of enzyme kinetic parameters. Physical properties of the device, including volume and pore size, can be controlled and allow for a defined flux of reagents, diffusional mixing, and containment of enzymes within the device, without the need for tethering. Single and coupled enzyme reactions involving horseradish peroxidase (HRP) and glucose oxidase (GOX) are demonstrated. Using the fluorogenic substrate Amplex® Red, sensitive, real-time monitoring of glucose concentration and enzyme catalysis is possible. The platform is arrayable and has potential application for assessing enzyme variants, screening enzyme substrates and biosensing.

II. MATERIALS AND METHODS

Device Fabrication

The small volume reaction containers were fabricated as previously described in Retterer et al [27]. Briefly, the reaction vessels and microfluidic network were patterned through a combination of electron beam and optical lithography. Cryogenic etching was then used to simultaneously create the vessels and the microfluidic channels. The individual reaction containers and the microfluidic channel are etched to the same depth (~15 μm). The resulting silicon wafer contains 8 identical chips. Each chip is 4 cm long and consists of 2 channels, each with an array of 18 reaction containers with a volume of ~19 pL (Figure 1). The walls of the cylindrical reaction vessel are 2 μm thick and contain 56 slits. Individual

chips were subjected to 4, 5, 6, or 7 minute duration of plasma enhanced chemical vapor deposition (PECVD) of silicon dioxide to further reduce the pore size. The resulting slits range in size from ~5-200 nm wide and are ~10 μm deep [27-29].

After the small volume containers were loaded, the chip was covered with a 5 mm thick layer of polydimethyl siloxane (PDMS), which was used to seal the device. Sylgard 184 silicone elastomer kit (Fischer Scientific) was used to prepare PDMS. Sylgard 184 silicon base and the curing agent were mixed in a Petri dish at a 10:1 w/w ratio, respectively. The mixture was degassed for ~30 min and cured in the oven at 70°C for 60- 90 minutes. After baking, PDMS was cut into pieces covering the chip and two holes were punched on each end of the channel using an 18 gauge blunt tip needle. Polyethylene tubes were fitted into the holes to allow for the input and output of solutions from the channel.

Functional assessment of transport and molecular containment

Devices that had undergone 4, 5, 6 or 7 minutes PECVD were filled with fluorescein to determine the functional pore size of the devices. Prior to the experiments, the inner walls of the reaction device were treated with 1 mg/mL Bovine Serum Albumin (BSA) in PBS for 60 min to prevent nonspecific absorption of reagents to the surface of the device. The solutions were loaded into a glass micropipette with tip diameter of 2 μm (World Precision Instruments, TIP2TW1), using a flexible polyimide needle (World Precision Instruments). The cell mimic device was filled by touching the tip of the glass micropipette into the center of the device. The channel was filled with tris(hydroxymethyl)aminomethane (TRIS) buffer, which was flowed under a steady flow of 10 μL/h. The fluorescent devices were imaged at time intervals of 10 seconds. Devices with no pores, filled with fluorescein and imaged the same way as the other devices, were used as controls to account for photobleaching that can occur during imaging.

Immediately after the channel was filled with working solution, fluorescence was monitored by measuring the intensity from time lapse images taken every 10 seconds using an exposure time of 256 ms. A Zeiss Axioskop 2 FS Plus epifluorescent microscope equipped with a Retiga firewire camera, a 40x dry objective (Zeiss), and a 200 W mercury arc lamp was used to obtain the images. The Retiga firewire camera was synchronized with a Lambda SC smart shutter (Sutter, CA) and the proper filter sets were used to minimize photobleaching of resorufin during the experiments. The images were acquired as 16-bit grayscale TIFFs using acquisition software IPLab 4.0.8 (Scanalytics,Inc.). Camera settings, exposure times and binning were kept the same for all experiments in order to allow comparisons. Image intensity values for each of the reaction vessels were calculated and plotted using MATLAB (V7.2, MathWorks). Prism Statistical Software 5.0 (GraphPad Software Inc.) was used to analyze and graph the data. This software uses a nonlinear regression fitting to find the best-fit values of the experimental parameters by using the method of Marquardt and Levenberg. It utilizes a linear descent in early iterations and then gradually switches to the Gauss-Newton approach.

Enzyme Reactions

An Amplex Red Hydrogen Peroxide/Peroxidase Assay Kit (Invitrogen A22188) was used for monitoring the enzyme reaction experiments and used according to the manufacturer's directions. Several difficulties such as overflowing, quick sample drying and air bubble formation were encountered while loading the reaction containers. These difficulties are attributed to the small volume of the container (~19 pL) and were addressed by adjusting the viscosity of the reaction mix. Different ratios of reaction mix to glycerol were examined and a 10% glycerol solution was found to be optimal. The increased viscosity made device loading easier, lessened air bubble formation, and reduced evaporation before device sealing

with PDMS. Arrays of up to 18 devices could be prepared in this manner and only a brief amount of time (~20 minutes) was needed to prepare the reaction mix, load the device and begin measurements. Solutions containing different horseradish peroxidase (HRP) concentrations (0.025 U/mL, 0.25 U/mL and 2.5 U/mL) were mixed in a 1:1 ratio with 20 % glycerol. Several reaction vessels were filled with just 1x buffer and served as negative controls. The channel was then filled with working solution and kept at a constant flow rate of either 1, 5, 10 or 20 μL/hr. The working solution consisted of 100 μM Amplex Red, 5μM hydrogen peroxide (H_2O_2), 0.05 M sodium phosphate pH 7.4 and 10% glycerol. The experiments were conducted at room temperature and repeated a minimum of three times.

A similar procedure was followed for coupled enzyme reactions and used an Amplex® Red Glucose/Glucose Oxidase Assay Kit (Invitrogen A22189) according to manufacturer's directions. For these experiments, a solution containing 0.5 U/mL glucose oxidase and 0.5 U/mL horseradish peroxidase was mixed in a 1:1 ratio with a 20 % glycerol solution. Several devices were filled with either 0.25 U/mL HRP or GOX and used as negative controls. The chip was then covered with PDMS and the channel was filled with working solution at a constant flow rate of 10μL/hr. The working solution consisted of 100 μM Amplex® Red, 0.05 M sodium phosphate pH 7.4, 10% glycerol and either 0.01, 0.1, 1, 5, 10 or 100 mM glucose. GOX and HRP enzyme concentrations of 0.025 U/mL, 0.25 U/mL and 2.5 U/mL, corresponding to ~5×10^{-10}, 5×10^{-9} and 5×10^{-8} U/reaction vessel, repectively, were evaluated for optimizing the enzyme reaction rate. Devices that had undergone 7 min PECVD were chosen for the majority of experiments, as the pores were found small enough to contain the enzymes within the vessel. Each experimental condition was repeated in triplicate. Fluorescence monitoring of the experiment was performed as described above. Additionally, background fluorescence was measured for each reaction and was subtracted from the fluorescence intensity measured in the device.

For comparison, coupled enzyme reactions were also conducted in Costar 96 flat bottom well plates. The enzyme, substrate and glycerol concentrations were kept the same as in the microreaction vessels, and the final reaction volume in the plate well was 100 μL. Fluorescence was measured every 10 seconds using a Perkin Elmer HTS 7000 Plus BioAssay Reader. To ensure proper mixing of the reagents, the plate was shaken before each reading. Each experiment was repeated in triplicate.

RESULTS AND DISCUSSION

Effective determination of membrane pore size

To control the ability of the device to allow small molecules such as amplex red, glucose and resorufin to diffuse through the membrane while preventing or limiting large molecules such as glucose oxidase and horseradish peroxidase from diffusing out, plasma enhanced chemical vapor deposition (PECVD) was used to decrease the width of the pores. Electron microscopy and ion beam milling experiments indicate that oxide deposits at a rate of 60 nm/min on a flat horizontal surface and that the limiting aperture that results from 7 minutes of PECVD is on the order of ~10 nm [29]. However, the pore is irregularly shaped. An effective pore size was experimentally determined by measuring diffusive transport across the membrane. Fluorescein was used as a model small molecule and loaded into vessels coated for 4, 5, 6, or 7 minutes with silicon dioxide by PECVD. Fluorescein diffusion out of devices was clearly dependent on PECVD time (Figure 2). These experimental data can be evaluated to determine an effective pore size by comparing the fluorescein diffusion results to a diffusion-based transport model. A Lumped Capacitance Model, based on Fick's law of diffusion, was used to predict transient changes in concentration within a nanoporous reaction vessel [27].

$$\Delta C = \frac{-Dnh_p w_p}{V\Delta x}(C_{in} - C_{out})\Delta t$$

D is the diffusivity of the species of interest (fluorescein), n is the number of pores, h_p is the pore height, w_p is the pore width, C is concentration, V is the volume of the device and x is the thickness of the membrane. Therefore the concentration within the vessel for an arbitrary time $t+k\Delta t$ can be given as:

$$C_{in}^{t+k\Delta t} = C_{in}^{t}\left(1 - \frac{Dnh_p w_p \Delta t}{V\Delta x}\right)^{k}$$

The above equation was used to calculate the predicted normalized fluorescein concentration within the device as a function of time based on changes in an effective pore width. As shown in Figure 2, fluorescein diffusion from devices that were subjected to 4, 5, 6, and 7 minute duration of PECVD silicon dioxide depositions correspond to effective pore widths of approximately 35, 25, 13 and 9 nm respectively. Figure 2 also shows that the diffusion of green fluorescent protein (GFP) from devices that have undergone 7 minute of silicon dioxide deposition is ~10% over a 10 minute period. However, GFP diffusion from a device that was subjected to 7 minute duration of PECVD of silicon dioxide corresponds to effective pore width of 5 nm. This pore width differs slightly from the 9 nm effective pore width that was calculated based on fluorescein diffusion. Both measurements are in line with electron microscopy-based evaluation of pore width. These latter efforts have shown that devices that have undergone 7 minute PECVD have a pore width between 5-10 nm[29]. As GFP (MW=29 kDa) is significantly smaller than GOX (MW=160 kDa) or HRP (MW= 44 kDa), reaction vessels coated by a 7 minute duration of PECVD should largely contain the enzymes over the course of the experiment. Related efforts have shown such devices are capable of containing a range of protein sizes over many hours of use[30].

Enzymatic Reactions

Single enzyme reactions were conducted initially for the purpose of evaluating the efficacy of the device and for determining effective reaction conditions. These reactions were successfully carried out on all devices that had undergone different PECVD silicon dioxide deposition times. Amplex® Red penetrated through the slits of the container and was converted from colorless into the red colored resorufin by HRP in the presence of H_2O_2 (Figure 3). As expected, based on the diffusion experiments, resorufin diffused out of the container quickly, flooding the channel with red fluorescent signal for enzyme reactions conducted on devices containing 2, 4 and 6 min of deposited oxide. For these devices, it is likely that HRP diffuses from the device and leads to increased signal in the channel. In contrast, experiments using 7 min of deposited oxide showed the resorufin signal to build up only in the reaction vessel before diffusing from the container. The effective pore size of these devices is expected to contain HRP but allow transport of small molecules such as Amplex® Red, H_2O_2 and resorufin. Therefore, 7 min PECVD devices were used for the remainder of the experiments. Flow rates of 1, 5, 10 and 20 μL/hr were examined and 10 μL/ hr was found to be sufficient for preventing buildup of resorufin in the channel. Enzyme concentrations in the range of 0.025 U/mL to 2.5 U/mL did not affect the success of the experiment.

Coupled enzyme reactions were also successfully conducted in the small volume reaction containers. GOX was combined with HRP to allow for fluorescence monitoring of glucose concentration. In this reaction, glucose is converted by GOX, in the presence of oxygen, into

gluconolactone and hydrogen peroxide. The newly formed H_2O_2 reacts with Amplex® Red in the presence of HRP to form the fluorescent resorufin. For these experiments, glucose and amplex red were flowed through the channel and diffused through the slits of the vessel. Glucose concentrations were varied and the fluorescence response was substrate dependent with higher glucose concentrations increasing the enzyme reaction rate, which reaches a plateau and remains approximately constant above 10 mM glucose concentration (Figure 4). The product concentration within the vessel reached a peak signal value corresponding to a concentration of ~7 μM resorufin within ~3 minutes when the glucose concentration was 100 mM and ~10 minutes when glucose concentration was 10 μM. For comparison, the same coupled enzyme reactions conducted in the plate reader showed a much slower response time and reached a peak concentration value of 6 μM resorufin within ~5 minutes for a 100 mM concentration of glucose and ~30-40 minutes when glucose concentration was 10 μM.

The kinetic characteristics of glucose oxidase were evaluated by measuring the time dependent resorufin fluorescence signal. The Michealis-Menten equation was used:

$$V_0 = V_{max} [S] / (K_m + [S])$$

where V_0 is the initial rate of the enzyme reaction, *[S]* is the substrate concentration, V_{max} is the maximum rate which corresponds to the velocity of the reaction when the enzymes are saturated with substrate, and K_m is equivalent to the concentration of substrate needed for half the maximal velocity. The peak substrate dependent rate was determined for each glucose concentration from the slopes of normalized fluorescence intensities as a function of time.

As opposed to preparing a double reciprocal plot, the data are plotted directly and fit using nonlinear regression according to the method of Marquardt and Levenberg [31] (Figure 5). This approach improves the fit of data points collected at low substrate concentrations when compared to linear regression fits of a double reciprocal plot. Within the small volume reaction containers, GOX is observed to have a $K_m = 1.65 \pm 0.17$ mM and a $V_{max} = 67 \pm 1.5$ μM min^{-1}, whereas in the plate reader the enzyme is measured to have a $K_m = 0.75 \pm 0.04$ mM and a $V_{max} = 25 \pm 0.3$ μM min^{-1}. The low K_m value for both reactions indicates that the catalytic rate of the coupled enzyme reactions is limited by stoichiometric restrictions such as oxygen levels, glucose and enzyme concentrations. The K_m for glucose oxidase from *A. niger* with respect to oxygen has been reported to be 0.51 mM [32,33], which is a close value to the K*m* from the plate reader and indicates an oxygen-limited maximum catalytic rate.

When compared to the conventional measurements performed using a plate reader, the K_m and V_{max} values are increased for the small volume reactions. These differences can be attributed to differences in the reaction format. The plate reader is a closed system and consequently reaction byproducts are contained and can result in substrate depletion and product inhibition. Further, high glucose concentrations can lead to the buildup of H_2O_2, which can oxidize resorufin to nonfluorescent resazurin[34,35]. This can give the appearance of a decreased reaction rate. The nanoscale slits of the microscale reactor system allow continuous exchange of substrate and product. This exchange can be considerable. Considering the fluorescein diffusion data described above, a significant portion (>40%) of small molecules such as glucose and resorufin should exchange in the amount of time needed for the reaction signal to reach a maximal value. This exchange, coupled with the small volume of the reaction, helps to maintain substrate levels, reduce product inhibition and prevent mass diffusion limitations. However, product loss will need to be accounted for in order to accurately assess kinetic characteristics of the enzyme. Reaction assessment

using devices with varying numbers of pores and an appropriate ordinary differential equation model could facilitate accurate assessment of kinetic characteristics. The ability to control the number of pores, the pore length and the pore width allows for design of a broad range of exchange rates. This is distinct advantage of the described platform and would also allow for reaction vessel optimization for particular applications. These values can be tuned along with the reaction volume to facilitate enzyme characterization.

In comparison to conventional, plate-based screening of enzyme activity, the described platform uses greatly reduced amounts of reagents, allows for controlled containment, and microfluidic control of reagent streams. These features make the described nanoporous, picoliter volume containers ideally suited for characterizing enzyme kinetics, for screening enzyme variants in parallel or for evaluating the effects of enzyme inhibitors. To enable routine use of the platform, alternative approaches to manual device filling may be required. For example, robotic spotting tools can be adapted. Alternatively, for experiment requiring large numbers of replicates, devices and channels can be filled before sealing. Flushing free enzyme from the flow channel would then follow this step.

CONCLUSION

A nanoporous, picoliter volume container for carrying out enzymatic reactions under continuous flow conditions has been described. The format and construction approach of the enzyme microreactor system described here offer a number of practical advantages. The platform allows for: (1) fast mass transfer kinetics; (2) the integration of microfluidics to manipulate the surrounding environment; (3) the ability to integrate multiple reactors to facilitate comparisons and screening throughput; (4) the trapping of enzymes in their native form rather than tethering and (5) the integration of controlled nanometer-sized pores that allow for selective containment and exchange of materials. These advantages can facilitate a number of applications for small volume reactors and directly benefit pursuits in drug discovery and clinical diagnostics.

Acknowledgments

REFERENCES

1. Urban PL, Goodall DM, Bruce NC. Enzymatic microreactors in chemical analysis and kinetic studies. Biotechnol Adv. 2006; 24:42–57. [PubMed: 16055295]

2. D'Auria S, Lakowicz JR. Enzyme fluorescence as a sensing tool: new perspectives in biotechnology. Curr Opin Biotechnol. 2001; 12:99–104. [PubMed: 11167081]

3. Welch GR, Somogyi B, Damjanovich S. The role of protein fluctuations in enzyme action: a review. Prog Biophys Mol Biol. 1982; 39:109–146. [PubMed: 7048419]

4. Colacino F, Crichton RR. Enzyme thermostabilization: the state of the art. Biotechnol Genet Eng Rev. 1997; 14:211–277. [PubMed: 9188155]

5. Girelli AM, Mattei E. Application of immobilized enzyme reactor in on-line high performance liquid chromatography: a review. J Chromatogr B Analyt Technol Biomed Life Sci. 2005; 819:3–16.

6. Ma L, Gong X, Yeung ES. Combinatorial screening of enzyme activity by using multiplexed capillary electrophoresis. Anal Chem. 2000; 72:3383–3387. [PubMed: 10939417]

7. Gleason NJ, Carbeck JD. Measurement of enzyme kinetics using microscale steady-state kinetic analysis. Langmuir. 2004; 20:6374–6381. [PubMed: 15248725]

8. Baganz F, Matosevic S, Szita N. Fundamentals and applications of immobilized microfluidic enzymatic reactors. J Chem Technol Biot. 2011; 86:325–334.

9. Doktycz MJ, Simpson ML. Nano-enabled synthetic biology. Molecular Systems Biology. 2007; 3:125. [PubMed: 17625513]

10. Matosevic S, Lye GJ, Baganz F. Design and characterization of a prototype enzyme microreactor: quantification of immobilized transketolase kinetics. Biotechnol Prog. 2010; 26:118–126. [PubMed: 19927318]

11. Walde P, Ichikawa S. Enzymes inside lipid vesicles: Preparation, reactivity and applications. Biomolecular Engineering. 2001; 18:143–177. [PubMed: 11576871]

12. Karlsson M, et al. Biomimetic nanoscale reactors and networks. Annual Review of Physical Chemistry. 2004; 55:613–649.

13. Yamaguchi A, et al. Rapid fabrication of electrochemical enzyme sensor chip using polydimethylsiloxane microfluidic channel. Analytica Chimica Acta. 2002; 468:143–152.

14. Vriezema DM, et al. Self-assembled nanoreactors. Chemical Reviews. 2005; 105:1445–1489. [PubMed: 15826017]

15. Mao H, Yang T, Cremer PS. Design and characterization of immobilized enzymes in microfluidic systems. Anal Chem. 2002; 74:379–385. [PubMed: 11811412]

16. McMullen JP, Jensen KF. Integrated Microreactors for Reaction Automation: New Approaches to Reaction Development. Annu Rev Anal Chem. 2010; 3:19–42.

17. Pijanowska DG, et al. The pH-detection of triglycerides. Sensor Actuat B-Chem. 2001; 78:263–266.

18. Jung SY, Liu Y, Collier CP. Fast mixing and reaction initiation control of single-enzyme kinetics in confined volumes. Langmuir. 2008; 24:4439–4442. [PubMed: 18361535]

19. Hadd AG, Raymond DE, Halliwell JW, Jacobson SC, Ramsey JM. Microchip device for performing enzyme assays. Anal Chem. 1997; 69:3407–3412. [PubMed: 9286159]

20. Burke BJ, Regnier FE. Stopped-flow enzyme assays on a chip using a microfabricated mixer. Anal Chem. 2003; 75:1786–1791. [PubMed: 12713034]

21. Duffy DC, Gillis HL, Lin J, Sheppard NF, Kellogg GJ. Microfabricated centrifugal microfluidic systems: Characterization and multiple enzymatic assays. Analytical Chemistry. 1999; 71:4669–4678.

22. Seong GH, Heo J, Crooks RM. Measurement of enzyme kinetics using a continuous-flow microfluidic system. Anal Chem. 2003; 75:3161–3167. [PubMed: 12964765]

23. Tanaka Y, et al. Acceleration of an enzymatic reaction in a microchip. Anal Sci. 2001; 17:809–810. [PubMed: 11708110]

24. Nomura A, Shin S, Mehdi OO, Kauffmann JM. Preparation, characterization, and application of an enzyme-immobilized magnetic microreactor for flow injection analysis. Anal Chem. 2004; 76:5498–5502. [PubMed: 15362912]

25. Sakai-Kato K, Kato M, Toyo'oka T. Creation of an on-chip enzyme reactor by encapsulating trypsin in sol-gel on a plastic microchip. Anal Chem. 2003; 75:388–393. [PubMed: 12585462]

26. Holden MA, Jung SY, Cremer PS. Patterning enzymes inside microfluidic channels via photoattachment chemistry. Anal Chem. 2004; 76:1838–1843. [PubMed: 15053641]

27. Retterer ST, Siuti P, Choi CK, Thomas DK, Doktycz MJ. Development and fabrication of nanoporous silicon-based bioreactors within a microfluidic chip. Lab on a Chip. 2010; 10:1174–1181. [PubMed: 20390137]

28. Siuti P, Retterer ST, Choi CK, Fowlkes JD, Doktycz MJ. Cell Free Translation in Engineered Picoliter Volume Containers. 2009 First Annual Ornl Biomedical Science & Engineering Conference: Exploring the Intersections of Interdisciplinary Biomedical Research. 2009; 80-83:150.

29. Srijanto BR, Retterer ST, Fowlkes JD, Doktycz MJ. Nanostructured silicon membranes for control of molecular transport. J Vac Sci Technol B. 2010; 28

30. Siuti P, Retterer ST, Doktycz MJ. Continuous protein production in nanoporous, picoliter volume containers. Lab on a Chip. 2011

31. Gill PE, Murray W. Algorithms for Solution of Non-Linear Least-Squares Problem. Siam J Numer Anal. 1978; 15:977–992.

32. Boudrant J, Cheftel C. [Application of the theory of oxygen transfer: determination of the Michaelis constant of glucose oxidase with respect to oxygen]. Biochimie. 1975; 57:117–122. [PubMed: 1138970]

33. Zimmermann S, Fienbork D, Stoeber B, Flounders AW, Liepmann D. A microneedle-based glucose monitor: Fabricated on a wafer-level using in-device enzyme immobilization. Boston Transducers'03: Digest of Technical Papers, Vols 1 and 2. 2003; 99-102:1938.

34. Zhou M, Diwu Z, Panchuk-Voloshina N, Haugland RP. A stable nonfluorescent derivative of resorufin for the fluorometric determination of trace hydrogen peroxide: applications in detecting the activity of phagocyte NADPH oxidase and other oxidases. Anal Biochem. 1997; 253:162–168. [PubMed: 9367498]

35. Mohanty JG, Jaffe JS, Schulman ES, Raible DG. A highly sensitive fluorescent micro-assay of H2O2 release from activated human leukocytes using a dihydroxyphenoxazine derivative. Journal of Immunological Methods. 1997; 202:133–141. [PubMed: 9107302]
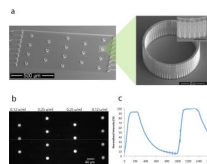
Figure 1.
A nanoporous, picoliter volume device platform for enzyme reactions. (a) SEM micrograph of a microfluidic device with an array of 18 reaction containers. The inset SEM micrographs show a single reaction container and a part of the container wall showing the nanoscale slits. After PECVD, the slits have a limiting aperture of ~10 nm. (b) A fluorescent micrograph of an array of enzyme reactions being carried out simultaneously. Enzyme concentrations of either 0.125 U/mL to 0.25 U/mL of glucose oxidase (GOX) and horseradish peroxidase (HRP) are contained in the devices and 10 mM glucose is flowed in the channel. (c) Time dependent trace of the normalized fluorescence intensity in a reaction container (0.25 U/mL GOX and 0.25 U/mL HRP) as flow is alternated between buffer with and without 10 mM glucose. Error bars representing +/- one standard deviation are shown at 50 seconds intervals for clarity.
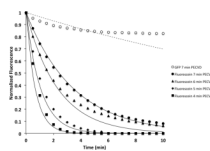
Figure 2.
Experimental diffusion data and diffusion model for devices that have undergone 4, 5, 6 and 7 minutes of PECVD. Solid data points correspond to the relative, average fluorescein intensity in the device and result from three diffusion experiments (3 individual devices on 3 separate chips). The solid lines correspond to the calculated fluorescein concentration using a Lumped Capacitance model and a pore size of either 9, 13, 25 or 35 nm. An increased duration of PECVD decreases the observed pore size of the device. For comparison, the open circles correspond to GFP diffusion data in a device coated with 7 minutes of PECVD, and the dashed line corresponds to a model of GFP diffusion using a 5 nm pore.
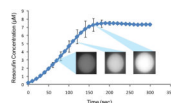
Figure 3.
Fluorescently measured single enzyme reaction in picoliter volume reactors. Devices that have undergone 7 min PECVD were filled with 0.25 U/mL horseradish peroxidase (HRP) and exposed to 2.5μM hydrogen peroxide (H_2O_2) using a constant flow rate of 10 μL/hr. Representative fluorescent micrographs of the cell mimic devices taken a different time points are shown. Error bars representing +/- one standard deviation of 3 individual devices on 3 separate chips are shown at 20 seconds intervals for clarity.
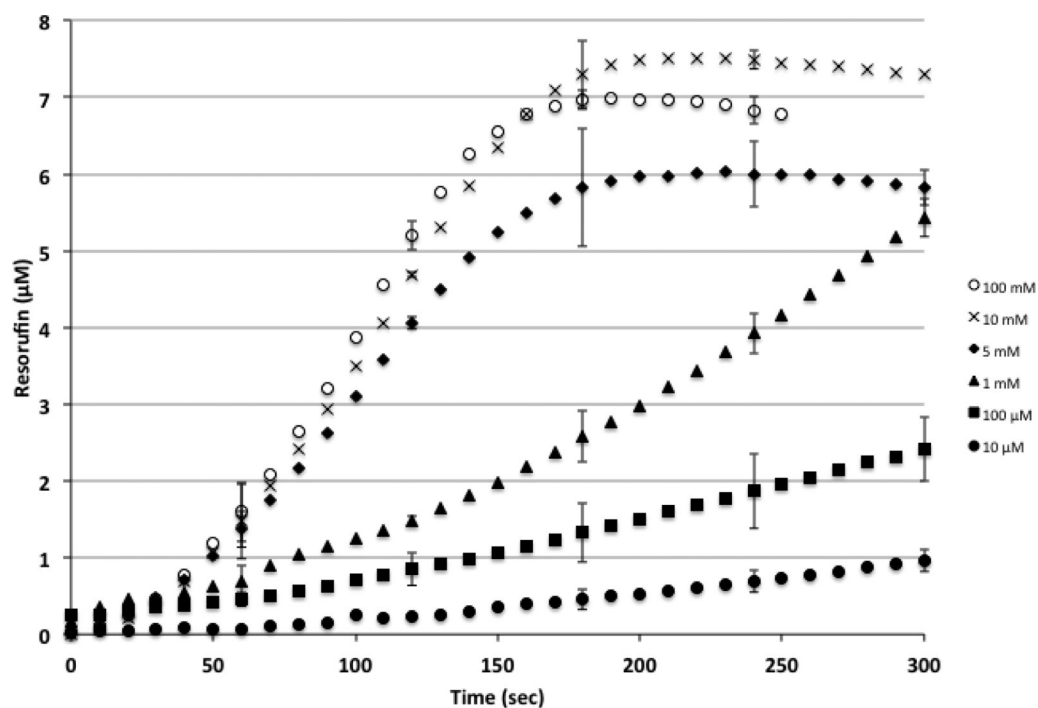
Figure 4.
Substrate dependent fluorescence response for coupled enzyme reactions in picoliter volume reactors. As glucose concentration increases from 10 μM to 100 mM, the rate of product formation, as measured by resorufin fluorescence, increases. Each data point represents the resorufin concentration, based on the observed fluorescence intensity, from three coupled enzyme reaction experiments (3 individual devices on 3 separate chips). Error bars represent +/- one standard deviation and are shown at 60-second intervals for clarity.
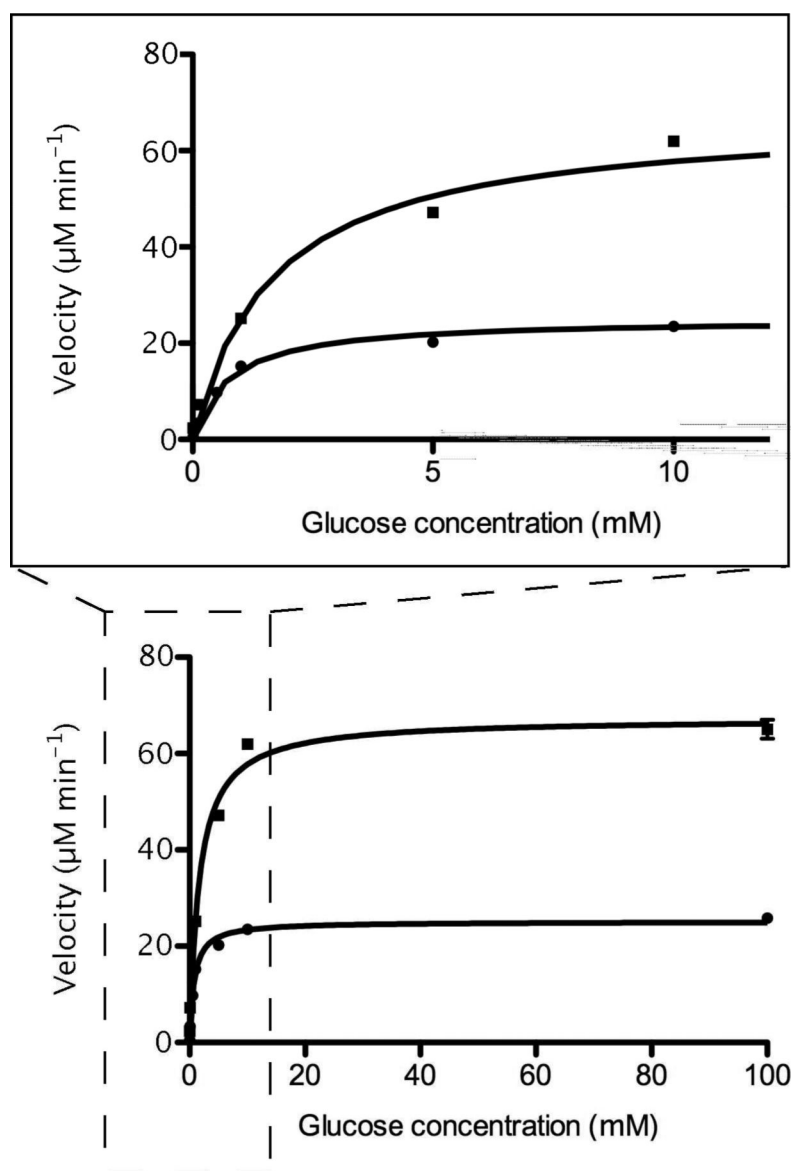
Figure 5.
Nonlinear regression fitting of Michealis-Menten plots of coupled enzyme reactions in picoliter volume reaction device (ν) and plate reader (λ). The K_m and V_{max} for the reaction device were found to be 1.65 ± 0.17 mM and 67 ± 1.5 μM min^{-1} respectively. For comparison, the K_m and V_{max} for the coupled enzyme reactions carried out in a plate reader (100 μL volume) were found to be 0.75 ± 0.04 mM and 25 ± 0.3 μM min^{-1} respectively. The inset expands the low glucose concentration region.